Proceedings of the 28th IEEE
EMBS Annual International Conference
New York City, USA, Aug 30-Sept 3, 2006

Nonrigid Registration of Images with Different Topologies using Embedded Maps

Christopher L. Wyatt, Member IEEE and Paul J. Laurienti

Abstract— **Changes in image topology occur in medical images due to normal variation in anatomy, image artifacts, and the presence of pathology. Non-rigid registration of images undergoing topological change for the purpose of atlas-based segmentation or deformation analysis is challenging since non-smooth geometric transformations must be introduced. As most registration methods impose a smoothness constraint on the allowable transformations they either do not model such changes or perform poorly in their presence. In this paper we describe an approach to non-rigid registration treating the images as embedded maps that deform in a Riemannian space. We show that smooth transformations representing topological changes in the original images can be obtained and describe the evolution in terms of a partial differential equation. Two-dimensional examples from brain morphometry are used to illustrate the method.**

I. INTRODUCTION

Image registration establishes a spatial correspondence between images and is a fundamental tool of medical image analysis. A fundamental limitation of non-rigid registration methods is in applications where there is a topological change in the level sets of the intensity image. In fact, many registration methods explicitly enforce topology preservation (e.g. [16]), reasoning that anatomical structures should have the same topology between any two individuals. While this assumption is valid in many cases, in studies of disease, and in certain populations such as the elderly, who are prone to changes in gray and white matter appearance, changes in topology are common and must be addressed. For example, the appearance of white matter lesions and their change in characteristics over time have been well documented in Multiple Sclerosis (MS) [18].

In this paper, we propose a representation for images and their deformation that includes both spatial geometry and intensity. The images are embedded as manifolds in a higher dimensional space. The deformation field between the images is defined as a transformation in the embedded space that matches the two manifolds. Using this approach, the geometric deformation and changes of intensity are coupled, leading to a natural accommodation of topology changes between the images.

C. Wyatt is with the Department of Electrical and Computer Engineering and the Virginia Tech - Wake Forest University School of Biomedical Engineering and Sciences, Virginia Tech, Blacksburg, VA 24061, USA clwyatt@vt.edu

P. Laurienti is with the Division of Radiologic Sciences - Radiology, Wake Forest University Health Sciences Winston-Salem, NC 27157, USA plaurien@wfubmc.edu

II. RELATED WORK

Many solutions to the registration problem have been developed, each with advantages and disadvantages. Recent reviews on registration provide an excellent framework in which to partition these methods including transform type, metrics, and optimization strategies [17], [22], [2], [14]. This paper focuses on nonrigid registration, which has applications in atlas-based segmentation [21], [12], [10] and in deformation-based morphometry [8], [1], [5]. By necessity we restrict our review of previous work to relevant non-rigid approaches.

The goal of nonrigid registration is to match anatomically meaningful regions by defining a geometric transformation with many degrees of freedom between images. Common representations for the transformation include splines [19], [15], kernels [9], and explicit vector fields [21]. Computation of the transformation may be classified as feature based, if an explicit detection of points or contours is used, or as a direct method, if the raw image data is used. Nonrigid registration methods based on features are robust to large deformations, but are limited by the detection accuracy and correspondence requirements, and are not considered here.

There are several approaches to direct nonrigid registration. A large class of methods are based on the optimization over the set of transformations of a matching metric. Metrics that have been studied include normalized cross correlation and those based on information theory. The sometimes difficult optimization of these and other metrics have been studied extensively. Another class of methods define a partial differential equation (PDE) describing the deformation. This approach has also been studied broadly, leading to e.g. the demons algorithm [20], fluid registration [4], curvature based registration [11], and level set motion [21].

As noted by Cuzol et al.[7], the regularization of the deformation field imposed by many registration approaches requires the deformation fields to have zero vorticity and divergence, preventing them from representing topological changes. To model fields with non-zero vorticity and divergence they introduce discrete vortex particles. This approach leads to a difficult optimization problem and requires a non-trivial extension to 3D images.

In contrast to [7] we observe that many PDE-based registration methods can represent divergent fields, but require the constant brightness assumption to hold at least approximately. However, topological changes can introduce drastic intensity changes. This causes PDE-based schemes that assume approximate constant intensity to perform poorly

1-4244-0033-3/06/$20.00 ©2006 IEEE.

in those areas.

The method we propose couples the intensity and geometric changes between images by embedding them as manifolds in a higher dimensional space. The consequence of this embedding is that a smooth geometric transformation between the images can be found, yet still accommodate (and represent) topological changes. Similar representations have been used as a unifying framework in image enhancement [13]. The use of higher dimensional representations also appears in the fluid registration algorithms (e.g. [4]), but differs from our approach in that the embedding is in time rather than intensity.

III. REGISTRATION USING EMBEDDED MAPS

In this section we describe the deformation of a *source* image, $I_S(x,y)$, to a *target* image, $I_T(x,y)$, through a transform centered in the target image, $I(x,y) = I_S(x-u, y-v) - w$, where u and v are the spatial displacements and w is an intensity displacement. The displacements can be collected into a vector $\vec{V} = [u \ v \ w]^T$. Because any two images can be related by a trivial intensity displacement ($w = I_T - I_S$), we wish to restrict the amount of intensity change during the registration process. In our approach this restriction is accomplished by coupling the intensity and spatial displacements in a Riemannian space.

While the approach is applicable to N dimensional, multi-channel images, we treat the single channel, 2D case here. First, we embed the images as a manifold in a Riemannian space with a suitably defined metric and describe some necessary geometric properties. We then describe the deformation of one manifold to another through a partial differential equation.

A. Images as embedded manifolds

Consider a two dimensional, single channel image $I(x,y) : \mathbb{R}^2 \mapsto \mathbb{R}$. The image can be embedded as a manifold in a 3D space through a mapping $X : \mathbb{R}^2 \mapsto \mathbb{R}^3$ where

$$x^1 = X^1(x,y) = x \tag{1}$$
$$x^2 = X^2(x,y) = y \tag{2}$$
$$x^3 = X^3(x,y) = I(x,y) \ . \tag{3}$$

The Riemannian metric or first fundamental form is used to measure distance on the surface, X, and is given by:

$$ds_X^2 = g_{x,x}dxdx + g_{x,y}dxdy + g_{y,x}dydx + g_{y,y}dydy \tag{4}$$

where the metric tensor is defined by

$$g_{\alpha,\beta} = \sum_{i=1}^{3}\sum_{j=1}^{3} h_{i,j}\frac{\partial X^i}{\partial \alpha}\frac{\partial X^j}{\partial \beta} \ . \tag{5}$$

We adopt an *anisometric* embedding since the intensity is in general of a different scale than the (x,y) coordinates, such that

$$h = \begin{bmatrix} 1 & 0 & 0 \\ 0 & 1 & 0 \\ 0 & 0 & \sigma^2 \end{bmatrix} \tag{6}$$

for scale $\sigma \in \mathbb{R}^+$.

The choice of the embedding parameter σ in the current implementation depends on the intensity magnitudes in the images and is adjusted experimentally such that the intensity portion of the flow does not dominate. In applications where the signal intensity is approximnately known, the σ paramter can be fixed.

Using this embedding the metric components are

$$g_{x,x} = 1 + \sigma^2 I_x^2 \tag{7}$$
$$g_{x,y} = g_{y,x} = \sigma^2 I_x I_y \tag{8}$$
$$g_{y,y} = 1 + \sigma^2 I_y^2 \ . \tag{9}$$

The normal at any point p on the manifold is given by

$$\vec{U_p} = \frac{\vec{X_x} \times \vec{X_y}}{\sqrt{g_{x,x}g_{y,y} - g_{x,y}g_{x,y}}} = \frac{\begin{bmatrix} -\sigma I_x & -\sigma I_y & 1 \end{bmatrix}^T}{\left(1 + \sigma^2 I_x^2 + \sigma^2 I_y^2\right)^{\frac{1}{2}}} \ . \tag{10}$$

B. Manifold evolution

Given an embedding of the source and target images, we want to deform the source manifold to the target. While there are several choices that could be made at this point, here we define the evolution the the source manifold simply as

$$\frac{\partial X}{\partial t} = \phi \vec{U} \ . \tag{11}$$

The rationale for this choice is that we want the manifold to deform in its normal direction with a given speed, ϕ.

Equation (11) describes the evolution of the manifold as a non-rigid transformation of the image coordinates and an intensity transformation. The initial manifold at $t = 0$ is the embedded source image, i.e. $X(t=0) = X_S$. In the non-rigid registration application we want the source embedding to evolve to the target embedding so that the manifolds are identical. Thus, a natural representation for the speed function is

$$\phi(\vec{x}) = I_T - I(t) \ , \tag{12}$$

where $I(t)$ is the intensity coordinate of the evolving manifold at time t.

The deformation field, $\vec{V}(x,y)$ is tracked as the evolution of the geometric and intensity coordinates. Thus, the field is defined on a 2D plane but defines a 3D deformation, i.e. $V : \mathbb{R}^2 \mapsto \mathbb{R}^3$. The projection of $\vec{V}$ onto the image plane determines the geometric portion of the transformation. The intensity component of the vector describes the amount of deformation caused by changes to the intensity. Substituting the definition normal from equation (10) gives the PDE describing the evolution of the displacements

$$\begin{bmatrix} u(t) \\ v(t) \\ w(t) \end{bmatrix} = \frac{-(I_T - I(t))}{(1 + \sigma^2 I_x^2 + \sigma^2 I_y^2)^{\frac{1}{2}}} \begin{bmatrix} -\sigma I_x \\ -\sigma I_y \\ 1 \end{bmatrix} \tag{13}$$

We note that the *spatial components* of the PDE used in Equation 13 is similar to that in [21]. However, because the deformation in Equation 13 includes an intensity deformation, there is no constant brightness restriction between the images.

C. Numerical Implementation

We use an explicit method to approximate the non-linear hyperbolic PDE in equation (13). A min/mod finite difference scheme is used to approximate the derivatives of the current image as in [21]. The min/mod finite difference preserves the min/max of the equation and improves the stability of the evolution. A Gaussian filter, G, with a variance of 1.0 is used to reduce the sensitivity of the derivatives to noise. We define the discrete image as $I_{i,j}$, and the forward and backward derivative operators of the filtered image, $F = G * I$, with a shorthand notation as

$$F_x^+ = \frac{F_{i+1,j} - F_{i,j}}{\Delta x} \ , \ F_x^- = \frac{F_{i,j} - F_{i-1,j}}{\Delta x} \tag{14}$$

$$F_y^+ = \frac{F_{i,j+1} - F_{i,j}}{\Delta y} \ , \ F_y^- = \frac{F_{i,j} - F_{i,j-1}}{\Delta y} \ . \tag{15}$$

The min/mod function is given by

$$m(\alpha, \beta) = \begin{cases} \text{sign}(\alpha)\text{min}(|\alpha|, |\beta|), & \text{if } \alpha\beta > 0 \\ 0, & \text{if } \alpha\beta \leq 0 \end{cases} \ . \tag{16}$$

The final discretized equation is then

$$\begin{bmatrix} u_{i,j}^{k+1} \\ v_{i,j}^{k+1} \\ w_{i,j}^{k+1} \end{bmatrix} = \begin{bmatrix} u_{i,j}^{k} \\ v_{i,j}^{k} \\ w_{i,j}^{k} \end{bmatrix} + \Delta t \cdot S \begin{bmatrix} -\sigma m(F_x^+, F_x^-) \\ -\sigma m(F_y^+, F_y^-) \\ 1 \end{bmatrix} \tag{17}$$

where k is the iteration number and

$$S = \frac{-G * (I_T - I_{i,j}^k)}{(1 + \sigma^2 m(F_x^+, F_x^-)^2 + \sigma^2 m(F_y^+, F_y^-)^2)^{\frac{1}{2}}} \ . \tag{18}$$

The time step of the evolution was adapted at each iteration using

$$\Delta t \leq \frac{1}{4 \max(|\phi|)/\|U\|)} \ . \tag{19}$$

The stopping criteria was based on the mean-square of the update, stopping when the change in mean-square difference of the deformed image and target image difference was below a fixed level of $\epsilon = 0.01$. The embedding scaling was left as a free parameter.

IV. IMPLEMENTATION RESULTS

We present results from three different experiments to demonstrate the topological flexibility of the algorithm and its ability to recover large deformations. In the first experiment, the registration using embedded maps was compared to the results from the level set motion algorithm using a simple synthetic image. In the second experiment the registration using embedded maps was applied to a simulated brain image undergoing both mass preserving deformation and a topological change. The last experiment demonstrates the approach in real 2D images.

In the first experiment, a 256 x 256 synthetic image (Figure 1(a)) was deformed at opposite corners and a topological change introduced to produce the target image (Figure 1(b)). The level set motion algorithm of Vemuri et al. [21] was applied to register the images using the implementation provided in the Insight Segmentation and Registration Toolkit (www.itk.org). The standard deviation of the level set motion algorithm was adjusted to give the best segmentation results (4.0 standard deviations). Figure 1(c) shows the resulting deformation field for the level set motion algorithm. Note that while the deformation field indicates that the intensities in the center are increasing, it does so by "pulling" intensities from a large portion of the image. This leads to overly smooth deformation maps in the case of topological change. Figure 1(d) shows the 2D projection of the deformation map resulting from the use of embedded map registration. An intensity scaling parameter of $\sigma = 1.0$ was used. Since the image intensities are modified during the evolution, the algorithm is able to represent the topological change in the center as well as the deformations at the edges without overly smoothing the deformation field.

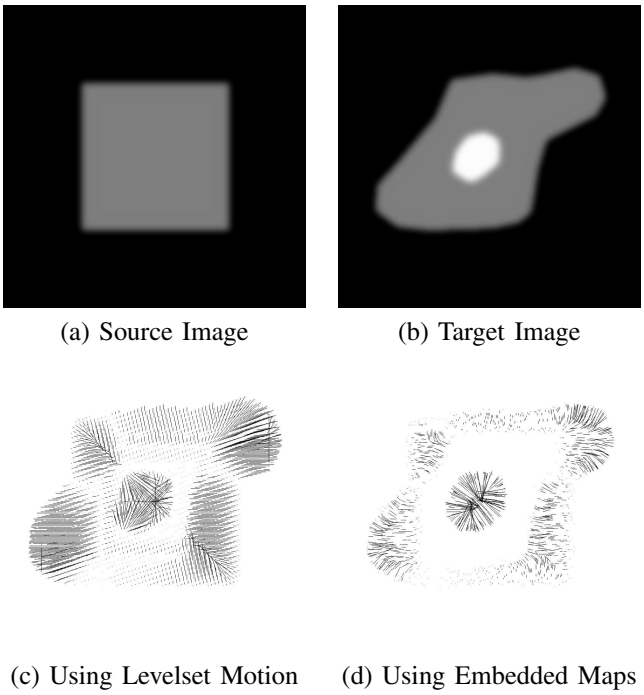

(a) Source Image (b) Target Image

(c) Using Levelset Motion (d) Using Embedded Maps

Fig. 1. An example of the deformation recovered in the case of a topological change from two algorithms. (a) Source image, (b) Target image, (c) deformation field from the level set motion algorithm (see text), (d) 2D projection of the deformation field from the algorithm described using embedded maps.

In the second experiment, corresponding slices from the normal and MS digital brain phantom (McConnell Brain Imaging Centre at McGill University [6]) were used. An additional non-rigid deformation was introduced in the MS image at several locations to mimic a mass preserving structural change in addition to the topological change from the lesions. Figures 2(a) and 2(b) show the source and target images respectively. The images were registered using the embedded map PDE with an intensity scaling factor of $\sigma = 0.1$. Figures 2(c,d) show the square error before and after the registration. Figure 2(e) shows the projection of the deformation field onto the image plane, with a detail around some of the simulated lesions in Figure 2(g). The intensity part of the deformation is shown in Figure 2(f). From the

detail, we can see the lesion is compactly represented by the deformation field.

To test the algorithm in real images, two sequential FLAIR images from an MS patient were rigidly co-registered and a corresponding slice form both volumes extracted (Figures 3(a) and 3(b)). The time between the image acquisitions was approximately six months. During this time, the lesions in the Parietal lobe have increased in intensity and size, as indicated in the deformation map (Figure 3(g)).

V. CONCLUSIONS AND FUTURE WORK

In this paper we have developed a registration algorithm for images with changing topology by representing the images as embedded manifolds and deriving a PDE flow to register the maps. Experiments based on simulations and real images demonstrate registration in the presence of lesion-like appearance or disappearance of material.

We note that the approach presented here is general and that there are additional choices for defining the flow between the manifolds. In particular the speed function ϕ in Equation 11 can be extended to depend on the distance to the nearest isocontour in the image, or to include shape or other priors.

A consequence of this approach, yet to be investigated, is how to simplify the information provided by the deformation map. In our case, the Jacobian of the deformation is not square and so has no determinant, the traditional means of measuring the deformation. However, the determinant of the Jacobian of the geometric portion of the deformation is square. Potential extensions include the ratio of this determinant and the magnitude of the intensity deformation as a way to highlight the location of the topology change.

VI. ACKNOWLEDGMENTS

This work was supported by the Virginia Tech - Wake Forest University School of Biomedical Engineering and Sciences seed grant program. P. Laurienti gratefully acknowledges the support of NIH grant # K08NS042568.

REFERENCES

[1] J. Ashburner, C. Hutton, R. Frackowiak, I. Johnsrude, C. Price, and K. Friston. Identifying global anatomical differences: Deformation-based morphometry. *Human Brain Mapping*, 6:348–357, 1998.

[2] L. G. Brown. A survey of image registration techniques. *Computing Surveys*, 24:325–376, 1992.

[3] V. Caselles, R. Kimmel, and G. Sapiro. Geodesic active contours. *Proc. 5th Int. Conf. Computer Vision*, 694–699, 1995.

[4] G. Christensen, R. Rabbitt, M. Miller. Deformable templates using large deformation kinetics *IEEE Transactions on Image Procesing*, 5(10):1435–1447, 1996.

[5] M. K. Chung, K. J. Worsley, T. Paus, C. Cherif, D. L. Collins, J. N. Giedd, J. L. Rapoport, and A. C. Evanst. A unified statistical approach to deformation-based morphometry. *Neuroimage*, 14:595–606, 2001.

[6] D.L. Collins and A.P. Zijdenbos and V. Kollokian and J.G. Sled and N.J. Kabani and C.J. Holmes and A.C. Evans: Design and construction of a realistic digital brain phantom. IEEE Trans. on Medical Imaging 17(3): 463-468 1998.

[7] M. Cuzol, P. Worsley, E. Mémin. A novel parametric method for non-rigid image registration. *LNCS 3565 (IPMI 2005)*, 456–467, 2005.

[8] C. Davatzikos. Measuring biological shape using geometry-based shape transformations. *Image And Vision Computing*, 19:63–74, 2001.

[9] M. H. Davis, A. Khotanzad, D. P. Flamig, and S. E. Harms. A physics-based coordinate transformation for 3-D image matching. *IEEE Transactions On Medical Imaging*, 16:317–328, 1997.

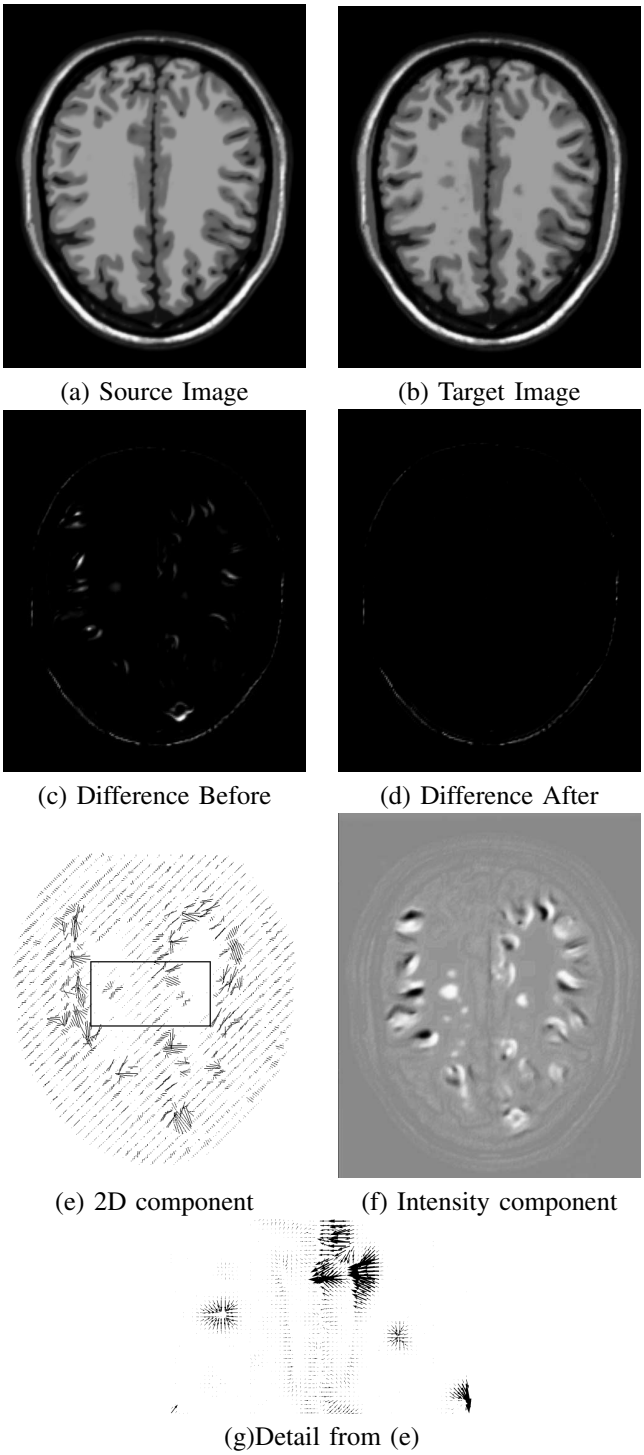

(a) Source Image (b) Target Image

(c) Difference Before (d) Difference After

(e) 2D component (f) Intensity component

(g)Detail from (e)

Fig. 2. Registration of simulated MR images in the presence of deformations and topological changes introduced by lesions. (a,b) Source and target images. (c,d) Square difference before and after registration. (e) Projection of the deformation onto the imaging plane. (f) Intensity component of the deformation (the min/max is -12.9/+11.8 % of max intensity). (g) Detail of (e) around the simulated lesions.

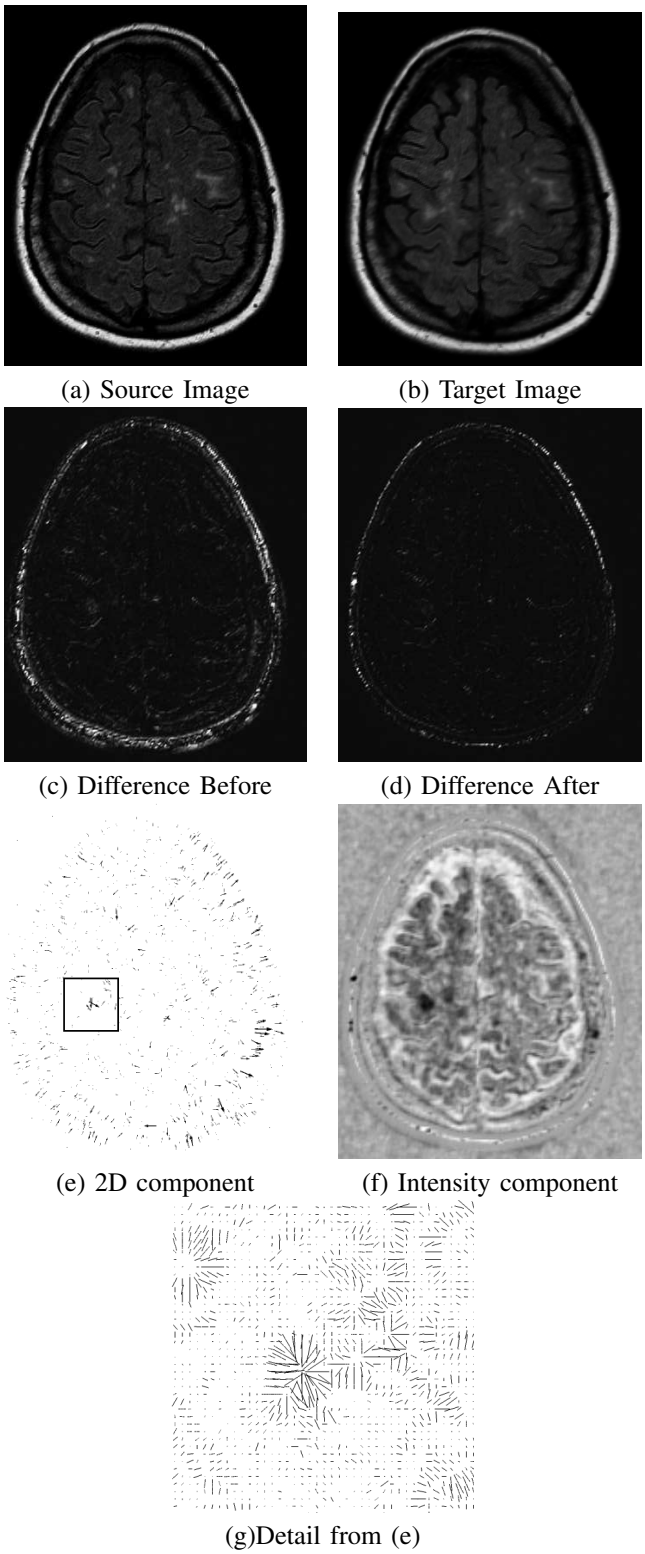

(a) Source Image (b) Target Image

(c) Difference Before (d) Difference After

(e) 2D component (f) Intensity component

(g)Detail from (e)

Fig. 3. Registration of MR images from a single patient in the presence of deformations and topological changes introduced by lesions. (a,b) Source and target images. (c,d) Square difference before and after registration. (e) Projection of the deformation onto the imaging plane. (f) Intensity component of the deformation. (g) Detail of (e) around the developing lesions.

[10] B. M. Dawant, S. L. Hartmann, J. P. Thirion, F. Maes, D. Vandermeulen, and P. Demaerel. Automatic 3-D segmentation of internal structures of the head in MR images using a combination of similarity and free-form transformations: Part I, methodology and validation on normal subjects. *IEEE Transactions On Medical Imaging*, 18:909–916, 1999.

[11] B. Fischer and J. Modersitzki. Curvature based image registration. *Journal of Mathematical Imaging and Vision*, 8 (1):81–85, 2003.

[12] S. L. Hartmann, M. H. Parks, P. R. Martin, and B. M. Dawant. Automatic 3-D segmentation of internal structures of the head in MR images using a combination of similarity and free-form transformations: Part II, validation on severely atrophied brains. *IEEE Transactions On Medical Imaging*, 18:917–926, 1999.

[13] R. Kimmel, R. Malladi, and N. Sochen. Images as embedded maps and minimal surfaces: movies, color, texture, and volumetric medical images. *Int. Journal of Computer Vision*, 39(2):111–129, 2000.

[14] H. Lester and S. R. Arridge. A survey of hierarchical non-linear medical image registration. *Pattern Recognition*, 32:129–149, 1999.

[15] D. Mattes, D. R. Haynor, H. Vesselle, T. K. Lewellen, and W. Eubank. PET-CT image registration in the chest using free-form deformations. *IEEE Transactions On Medical Imaging*, 22:120–128, 2003.

[16] V. Noblet, C. Heinrich, F. Heitz, J. Armspach. 3-D deformable image registration: a topology preservation scheme based on hierarchical deformation models and interval analysis optimization. *IEEE Transactions on Image Processing*, 14(5):553–566, 2005.

[17] J. P. W. Pluim, J. B. A. Maintz, and M. A. Viergever. Mutual-information-based registration of medical images: A survey. *IEEE Transactions On Medical Imaging*, 22:986–1004, 2003.

[18] P. M. Pretorius and G. Quaghebeur. The role of MRI in the diagnosis of MS. *Clinical Radiology*, 58:434–448, 2003.

[19] D. Rueckert, L. I. Sonoda, C. Hayes, D. L. G. Hill, M. O. Leach, and D. J. Hawkes. Nonrigid registration using free-form deformations: Application to breast MR images. *IEEE Transactions On Medical Imaging*, 18:712–721, 1999.

[20] J. P. Thirion. Image matching as a diffusion process: an analogy with maxwell's demons *Medical Image Analysis*, 2(3):243–260, 1998.

[21] B. C. Vemuri, J. Ye, Y. Chen, and C. M. Leonard. Image registration via level-set motion: Applications to atlas-based segmentation. *Medical Image Analysis*, 7:1–20, 2003.

[22] B. Zitova and J. Flusser. Image registration methods: a survey. *Image And Vision Computing*, 21:977–1000, 2003.